Inorg. Chem. **2006**, *45*, 4497−4507

Di-, Tri-, and Tetranuclear Zinc Hydroxamate Complexes as Structural Models for the Inhibition of Zinc Hydrolases by Hydroxamic Acids

David A. Brown, Noel J. Fitzpatrick,* Helge Müller-Bunz, and Áine T. Ryan

School of Chemistry and Chemical Biology, Centre for Synthesis and Chemical Biology, Conway Institute of Biomolecular and Biomedical Research, University College Dublin, Belfield, Dublin 4, Ireland

Received May 25, 2005

Attempts to produce Zn analogues of the structural model complexes $[M_2(\mu\text{-}O_2CR)_2(O_2CR)_2(\mu\text{-}H_2O)(tmen)_2]$ (M = Ni, Co, Mn; R = CH_3, $C(CH_3)_3$, CF_3) by the reaction of a series of zinc carboxylates with *N,N,N′,N′*-tetramethylethylenediamine (tmen), resulted in the mononuclear complexes $[Zn(OAc)_2(tmen)]$ (**1**) and $[Zn(crot)_2(tmen)]\cdot 0.5H_2O$ (**2**) for R = CH_3 and $(CH)_2CH_3$, respectively, and the dinuclear complexes $[Zn_2(\mu\text{-}piv)_2(piv)_2(\mu\text{-}H_2O)(tmen)_2]$ (**3**) and $[Zn_2(\mu\text{-}OAc_F)_2(OAc_F)_2(\mu\text{-}H_2O)(tmen)_2]$ (**4**) for R = $C(CH_3)_3$ and CF_3, respectively. In contrast to the analogous imidazole series, i.e., $[M_2(\mu\text{-}O_2CR)_2(O_2CR)_2(\mu\text{-}H_2O)(Im)_4]$ (M = Ni, Co, Mn; R = CH_3, $C(CH_3)_3$, CF_3), zinc carboxylates react with imidazole to give only the mononuclear complexes $[Zn(OAc)_2(Im)_2]$ (**5**), $[Zn(crot)_2(Im)_2]\cdot H_2O$ (**6**), $[Zn(piv)_2(Im)_2]\cdot 0.5H_2O$ (**7**), and $[Zn(OAc_F)_2(Im)_2]$ (**8**). Reaction of **1**, **2**, and **3** with either acetohydroxamic acid (AHA) or benzohydroxamic acid (BHA) gives the dinuclear complexes $[Zn_2(O_2CR)_3(R'A)(tmen)]$, where R′A = acetohydroxamate (AA) (**9**, **10**, **11**) or benzohydroxamate (BA) (**13**, **14**, **15**). In these complexes, the zinc atoms are bridged by a single hydroxamate and two carboxylates, with a capping tmen ligand on one zinc and a monodentate carboxylate bonded to the second zinc atom. This composition models closely the observed structure of the active site of the *p*-iodo-D-phenylalanine hydroxamic acid inhibited *Aeromonas proteolytica* aminopeptidase enzyme. In contrast, **4** reacts with AHA to give $[Zn_2(OAc_F)_3(tmen)_2(AA)]$ (**12**) with an additional tmen ligand so that both Zn atoms are 6-coordinate, whereas reaction with BHA gives the trinuclear complex $[Zn_3(OAc_F)_4(tmen)_2(BA)_2]$ (**16**). Reactions of **3** and **4** with glutarodihydroxamic acid ($GluH_2A_2$) produce the tetranuclear complexes $[Zn_4(piv)_6(tmen)_4(GluA_2)]$ (**18**) and $[Zn_4(OAc_F)_6(tmen)_4(GluA_2)]$ (**19**).

Introduction

Zinc is the second most abundant metal in the body, after iron, playing catalytic, structural, regulatory, and noncatalytic roles in enzymes and a structural role in zinc finger proteins.[1,2] With well over 300 structurally identified enzymes, it is the only metal found in representatives of all six International Union of Crystallography classes of enzymes, namely oxidoreductases, transferases, hydrolases, lyases, isomerases, and ligases.[3] The hydrolases are responsible for a large number of physiological functions and pathologies, e.g., neoplasms, inflammations, infections. In addition to Zn, the transition metals Ni, Co, and Mn also form dinuclear metallohydrolases.[4] Structurally, these enzymes contain a dinuclear metal active site featuring Zn(II), Ni(II), Co(II), and Mn(II) bridged by carboxylates and occur, respectively, in leucine aminopeptidase,[5] urease,[6] methionineaminopeptidase,[7] and arginase.[8] Significantly, zinc hydrolases are involved in bacterial resistance (deactivation of penicillin by metallo-β-lactamases) and cancer progression (matrix metalloproteinases).[2] As a result, their inhibitors are potential antibacterial and anticancer drugs.[9]

Hydroxamic acids are known inhibitors of the metallohydrolases.[9] Recent structural developments have increased

* To whom correspondence should be addressed. Telephone: +353-1-716-2495. Fax: +353-1-716-2127. E-mail: noel.fitzpatrick@ucd.ie.

(1) Auld, D. S. *BioMetals* **2001**, *14*, 271−313.
(2) Lipscomb, W. N.; Sträter, N. *Chem. Rev.* **1996**, *96*, 2375−2433.
(3) Galdes, A.; Vallee, B. L. *Metal Ions in Biological Systems*; Sigel, H., Ed.; Marcel Dekker: New York, 1983; Vol. 15, Chapter 1, p 1.
(4) Wilcox, D. *Chem. Rev.* **1996**, *96*, 2435−2458.
(5) Sträter, N.; Lipscomb, W. N. *Biochemistry* **1995**, *34*, 14792−14800.
(6) Jabri, E.; Carr, M.; Hausinger, R.; Karplus, P. *Science* **1995**, *268*, 998−1004.
(7) Roderick, S.; Matthews, B. *Biochemistry* **1993**, *32*, 3907−3912.
(8) Kanyo, Z.; Scolnick, L.; Ash, D.; Christianson, D. *Nature* **1996**, *383*, 554−557.
(9) Muri, E. M. F.; Nieto M. J.; Sindelar R. D.; Williamson, J. S. *Curr. Med. Chem.* **2002**, *9*, 1631−1653.

10.1021/ic050849m CCC: $33.50
Published on Web 05/02/2006

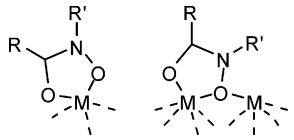

Figure 1. Modes of coordination of hydroxamate inhibitors to mononuclear sites (left) and dinuclear sites (right).

our knowledge of how hydroxamic acids bind to metal centers; however, the mechanisms are still a matter for debate. Inhibition of mononuclear centers involves chelation of the metal ion by the hydroxamate in the 'O,O' bonding mode, i.e., through the carbonyl oxygen and through the deprotonated hydroxyl oxygen (Figure 1). Crystal structures of many mononuclear zinc enzymes with coordinated hydroxamate inhibitors have been solved, e.g., DD-carboxypeptidase,[10] thermolysin,[11] neutrophil collagenase (matrix metalloproteinase-8),[12] fibroblast collagenase (matrix metalloproteinase-1),[13] and fuculose-1-phosphate aldose.[14] All examples show the hydroxamate chelating the metal center through both oxygens.

In dinuclear enzymes, inhibition occurs when the hydroxamate is coordinated so that it bridges both metal centers. Specifically, the carbonyl oxygen coordinates to the first metal center and the deprotonated hydroxamate oxygen bridges both metal centers (Figure 1). This coordination mode was initially observed in the model complex $[Ni_2(Hshi)(H_2shi)(pyr)_4(OAc)]$ (OAc = $CH_3CO_2^-$), which contains two bridging hydroxamates.[15] The crystal structures of acetohydroxamic acid bound to both *Klebsiella aerogenes* urease[16] and *Bacillus pasteurii* urease[17] show a single inhibitor molecule bound to the enzyme in the same mode as in $[Ni_2(Hshi)(H_2shi)(pyr)_4(OAc)]$. To the best of our knowledge, only one crystal structure of a dinuclear zinc enzyme with a bridged coordinated hydroxamate inhibitor is known, i.e., *Aeromonas proteolytica* aminopeptidase (Zn_2AAP) inhibited by *p*-iodo-D-phenylalanine hydroxamic acid (Figure 2).[18]

The complexes $[M_2(\mu\text{-}O_2CR)_2(O_2CR)_2(\mu\text{-}H_2O)(tmen)_2]$ (M = Ni, Co, Mn; R = CH_3, $C(CH_3)_3$, CF_3; tmen = *N*,*N*,*N*′,*N*′-tetramethylethylenediamine) consist of a dinuclear metal center with bridging carboxylates and a bridging water,[19−23] making them ideal candidates for structurally modeling the

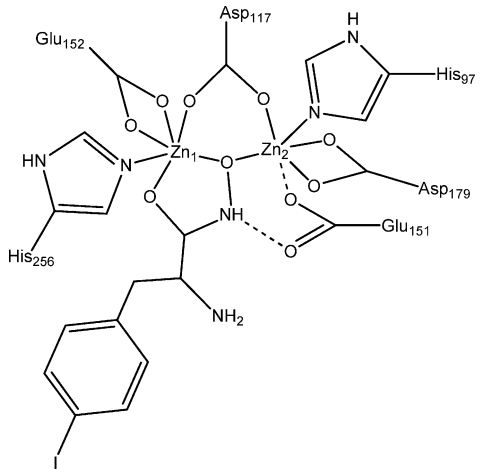

Figure 2. *Aeromonas proteolytica* aminopeptidase inhibited by *p*-iodo-D-phenylalanine hydroxamic acid.[18]

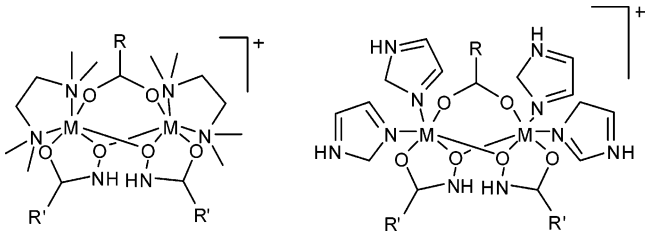

Figure 3. Model hydroxamate complex ions $[M_2(O_2CR)(R'A)_2(tmen)_2]^+$ (left) and $[M_2(O_2CR)(R'A)_2(Im)_4]^+$ (right).

dinuclear metallohydrolases which also contain a dinuclear active site bridged by the carboxylate end of an amino acid.[4] We have shown that reacting the dinuclear complexes $[M_2(\mu\text{-}O_2CR)_2(O_2CR)_2(\mu\text{-}H_2O)(tmen)_2]$ or $[M_2(\mu\text{-}O_2CR)_2(O_2CR)_2(\mu\text{-}H_2O)(Im)_4]$ (Im = imidazole) with 2 equiv of hydroxamic acid gives the hydroxamate complex $[M_2(O_2CR)(R'A)_2(tmen)_2][O_2CR]$ or $[M_2(O_2CR)(R'A)_2(Im)_4][O_2CR]$ (Figure 3), respectively, (M = Ni, Co, Mn; R = CH_3, $(CH_3)_3C$; R′A = acetohydroxamate, benzohydroxamate, *N*-phenylacetohydroxamate).[19−22] However, when R = CF_3 was used, different complexes were produced.[23] When either $[Ni_2(\mu\text{-}OAc_F)_2(OAc_F)_2(\mu\text{-}H_2O)(tmen)_2]$ (OAc_F = $CF_3CO_2^-$) or $[Co_2(\mu\text{-}OAc_F)_2(OAc_F)_2(\mu\text{-}H_2O)(tmen)_2]$ was reacted with 2 equiv of hydroxamic acid, a trinuclear complex of the form $[M_3(OAc_F)_4(tmen)_2(R'A)_2]$ was formed (Figure 4). Proton transfer to the tmen nitrogen atoms and formation of the doubly protonated salt, $[tmenH_2][OAc_F]_2$ with H-bonding between the protons and the trifluoroacetates, also occurred.[23]

(10) Charlier, P.; Dideberg, O.; Jamoulle, J. C.; Frère, J. M.; Ghuysen, J. M.; Dive, G.; Lamotte-Brasseur, J. *Biochem. J.* **1984**, *219*, 763−772.
(11) Holmes, M. A.; Matthews, B. W. *Biochemistry* **1981**, *20*, 6912−6920.
(12) (a) Stams, T.; Spurlino, J. C.; Smith, D. L.; Wahl, R. C.; Ho, T. F.; Qoronfleh, M. W.; Banks, T. M.; Rubin, B. *Nature, Struct. Biol.* **1994**, *1*, 119−123. (b) Grams, F.; Crimmin, M.; Hinnes, L.; Huxley, P.; Pieper, M.; Tschesche, H.; Bode, W. *Biochemistry* **1995**, *34*, 14012−14020. (c) Grams, F.; Reinemer, P.; Powers, J. C.; Kleine, T.; Pieper, M.; Tschesche, H.; Huber, R.; Bode, W. *Eur. J. Biochem.* **1995**, *228*, 830−841.
(13) Spurlino, J. C.; Smallwood, A. M.; Carlton, D. D.; Banks, T. M.; Vavra, K. J.; Johnson, J. S.; Cook, E. R.; Falvo, J.; Wahl, R. C.; Pulvino, T. A.; Wendoloski, J. J.; Smith, D. L. *Proteins* **1994**, *19*, 98−109.
(14) Dreyer, M. K.; Schulz, G. E. *J. Mol. Biol.* **1993**, *231*, 549−553.
(15) Stemmler, A. J.; Kampf, J. W.; Kirk, M. L.; Pecoraro, V. L. *J. Am. Chem. Soc.* **1995**, *117*, 6368−6369.
(16) Pearson, M.; Michel, L.; Hausinger, R.; Karplus, P. *Biochemistry* **1997**, *36*, 8164−8172.
(17) Benini, S.; Rypniewski, W. R.; Wilson, K. S.; Miletti, S.; Ciurli, S.; Mangani, S. *J. Biol. Inorg. Chem.* **2000**, *5*, 110−118.
(18) Chevrier, B.; D'Orchymount, H.; Schaik, C.; Tamus C.; Moras, D. *Eur. J. Biochem.* **1996**, *237*, 393−398.
(19) Brown, D. A.; Cuffe, L. P.; Deeg, O.; Errington, W.; Fitzpatrick, N. J.; Glass, W. K.; Herlihy, K. Kemp, T. J., Nimir, H. *Chem. Commun.* **1998**, 2433−2434.
(20) Arnold, M.; Brown, D. A.; Deeg, O.; Errington, W.; Hasse, W.; Herlihy, K.; Kemp, T. J.; Nimir, H.; Werner, R. *Inorg. Chem.* **1998**, *37*, 2920−2925.
(21) Brown, D. A.; Errington, W.; Glass, W. K.; Hasse, W.; Kemp, T. J.; Nimir, H.; Ostrovsky, S.; Werner, R. *Inorg. Chem.* **2001**, *40*, 5962−5971.
(22) Brown, D. A.; Glass, W. K.; Fitzpatrick, N. J.; Kemp, T. J.; Errington, W.; Clarkson, G. J.; Hasse, W.; Karsten, F.; Mahdy, A. H. *Inorg. Chim. Acta* **2004**, *357*, 1411−1436.
(23) Brown, D. A.; Clarkson, G. J.; Fitzpatrick, N. J.; Glass, W. K.; Hussein, A. J.; Kemp, T. J.; Müller-Bunz, H. *Inorg. Chem. Commun.* **2004**, *7*, 494−498.

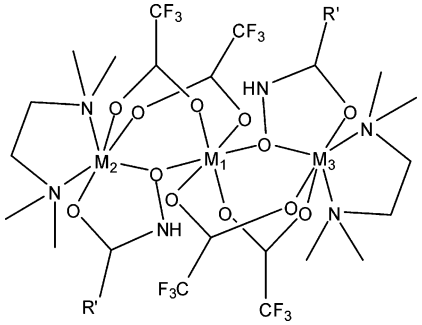

Figure 4. General structure of the trinuclear complex $[M_3(OAc_F)_4(tmen)_2(R'A)_2]$.

When either $[M_2(\mu\text{-}O_2CR)_2(O_2CR)_2(\mu\text{-}H_2O)(tmen)_2]$ or $[M_2(\mu\text{-}O_2CR)_2(O_2CR)_2(\mu\text{-}H_2O)(Im)_4]$ (where M = Ni or Co and R = CH_3 or $(CH_3)_3C$)) was reacted with 1 equiv of glutarodihydroxamic acid ($GluH_2A_2$), in the presence of a counterion, the ion $[M_2(O_2CR)\{\mu\text{-}O(N)(OC)_2(CH_2)_3\}(tmen)_2]^+$ was formed with the elimination of hydroxylamine.[19] Interestingly, when the urea complex $[M_2(O_2CR)_3(urea)(tmen)_2]$ was reacted with 1 equiv of $GluH_2A_2$, in the presence of a counterion, the tetranuclear ion $[M_4(O_2CR)_2(GluA_2)_2(tmen)_4]^{2+}$ ($GluA_2$ = glutarodihydroxamate) was formed.[19] The complex is composed of two dinuclear $[M_2(O_2CR)(0.5GluA_2)_2(tmen)_2]^{2+}$ units, linked by the aliphatic chains of the $GluA_2$'s. The general structure of each of the dinuclear units is similar to that of the $[M_2(O_2CR)(R'A)_2(tmen)_2]^{2+}$ complexes (Figure 3).[19]

With the exception of our preliminary communication,[24] in which the crystal structures of **1** and the product of its reaction with benzohydroxamic acid (BHA), **13**, were reported, such structures have not yet been reported for zinc for either the dinuclear model hydrolases or the bridged hydroxamate inhibited model hydrolases.

Results and Discussion

1. Structural Models for Zinc Hydrolases. The structural model complexes $[M_2(\mu\text{-}O_2CR)_2(O_2CR)_2(\mu\text{-}H_2O)(tmen)_2]$ (M = Ni, Co, Mn; R = CH_3, $C(CH_3)_3$, CF_3) are prepared by the reaction of the relevant metal carboxylate with tmen.[19−23] However, when zinc acetate or zinc crotonate $[Zn(CH_3(CH)_2CO_2)]$ was reacted with tmen, the mononuclear complexes **1**[24] or **2** were obtained instead (Figure 5), whereas with zinc pivalate and zinc trifluoroacetate, the dinuclear complexes **3** and **4** were formed, with similar structures to the analogous Ni, Co, and Mn dinuclear complexes (Figure 5). The model complexes $[M_2(\mu\text{-}O_2CR)_2(O_2CR)_2(\mu\text{-}H_2O)(Im)_4]$ (M = Ni, Co, Mn; R = CH_3, $C(CH_3)_3$, CF_3) also exist, prepared by the reaction of the relevant metal carboxylate with imidazole.[22,23] When the zinc carboxylates were reacted with imidazole, only the mononuclear complexes **5**, **6**, **7**, and **8** were produced (Figure 5).

Crystallographic data for **2**, **4**, and **6**−**8** are given in Table 1 with selected bond lengths and angles and ORTEP figures given in the Supporting Information. The previously reported[24] complex **1** is distorted octahedral with slight

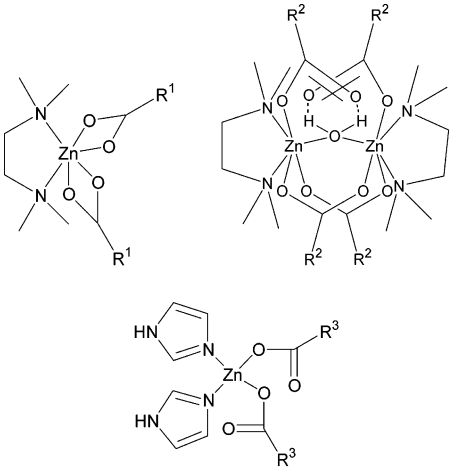

Figure 5. General structures of **1** (R^1 = CH_3), **2** (R^1 = $(CH)_2CH_3$), **3** (R^2 = $C(CH_3)_3$), **4** (R^2 = CF_3), **5** (R^3 = CH_3), **6** (R^3 = $(CH)_2CH_3$), **7** (R^3 = $C(CH_3)_3$), and **8** (R^3 = CF_3).

distortion of the metal−ligand angles from 90°. Although there is some asymmetry in the M−O distances, Zn1−O1 is 2.052(4) Å and Zn1−O2 is 2.353(4) Å; both acetates are clearly bidentate chelating. The complex **2** is also distorted octahedral with slight distortion of the metal−ligand angles from 90°. For example, ∠O1−Zn1−N1 is 102.32(13)° and ∠O2−Zn1−O2′ is 91.84(3)°. Although there is some asymmetry in the M−O distances, Zn1−O1 is 2.069(3) Å and Zn1−O2 is 2.299(4) Å; both crotonates are clearly bidentate chelating. These distances are shorter than those in **1**. A water molecule is shared between two complex molecules, hydrogen-bonded to O1 in both. The water is hydrogen-bonded to O1, which is the more tightly bound oxygen to the metal, thus indicating no tendency for the crotonate to become monodentate with hydrogen bonding to the water, as observed in the dinuclear complexes $[M_2(\mu\text{-}O_2CR)_2(O_2CR)_2(\mu\text{-}H_2O)(tmen)_2]$. The Zn−Zn separation is 8.064 Å.

1.1. X-ray Crystal Structure of the Dinuclear Complex 4. The crystal structure of **4** is shown in Figure 6 with selected bond lengths and angles in the Supporting Information. Both zinc atoms in **4** are octahedrally coordinated with only very slight deviation of the metal−ligand angles from 90°. The Zn1−Zn2 distance is 3.729 Å, and the ∠Zn1−O1−Zn2 angle is 116.41°. The M−M distance in **4** is significantly longer than that in the Ni and Co analogues, which are 3.676 and 3.702 Å, respectively.[23] The bond angles in **4** are quite similar to those in $[Co_2(\mu\text{-}OAc_F)_2(OAc_F)_2(\mu\text{-}H_2O)(tmen)_2]$.[23] The hydrogen bonds from the bridging water to the monodentate trifluoroacetates are unsymmetrical in **4** at (O1)H20···O7 1.79(3) and (O1)H10···O9 1.76(3) Å. Significantly, for the zinc complex, the average Zn−O bond length is 2.115 Å, much longer than 2.084 and 2.092 Å in the Ni and Co dinuclear complexes, respectively, reflecting how weakly the zinc dinuclear complex is held together.

1.2. Mononuclear Compounds 6−8. Crystallographic data for the three mononuclear complexes **6**−**8** can be found in Table 1 with selected bond lengths and angles and ORTEP diagrams given in the Supporting Information. Complex **5**

(24) Brown, D. A.; Errington, W.; Fitzpatrick, N. J.; Glass, W. K.; Kemp, T. J.; Nimir, H.; Ryan, A. T. *Chem. Commun.* **2002**, 1210−1211.

Table 1. Crystal Data and Structure Refinement for Compounds **2**, **4**, and **6**−**8**

	2	**4**	**6**	**7**	**8**
empirical formula	$C_{14}H_{28}N_2O_5Zn$	$C_{20}H_{34}N_4O_9F_{12}Zn_2$	$C_{14}H_{20}N_4O_5Zn$	$C_{16}H_{28}N_4O_5Zn$	$C_{10}H_8N_4O_4F_6Zn$
molecular formula	$C_{14}H_{26}N_2O_4Zn{\cdot}xH_2O$		$C_{14}H_{18}N_4O_4Zn{\cdot}xH_2O$	$C_{16}H_{26}N_4O_4Zn{\cdot}xH_2O$	
fw	369.75	833.25	389.71	419.78	427.57
T, K	293(2)	293(2)	100(2)	293(2)	293(2)
λ	0.71073	0.71073	0.71073	0.71073	0.71073
cryst syst	orthorhombic	monoclinic	monoclinic	monoclinic	monoclinic
space group	$C222_1$ (no. 20)	$P2_1/n$ (no. 14)	Pn (no. 7)	Pn (no. 7)	$P2_1/n$ (no. 14)
a, Å	9.280(3)	15.479(2)	7.9238(6)	13.487(2)	9.938(2)
b, Å	12.655(4)	13.889(2)	7.6937(6)	11.6785(17)	7.9370(18)
c, Å	15.761(4)	17.171(3)	14.8744(12)	13.487(2)	19.665(5)
α, °	90	90	90	90	90
β, °	90	114.268(2)	99.6220(10)	96.157(2)	99.642(4)
γ, °	90	90	90	90	90
V, Å^3	1850.9(9)	3365.1(9)	894.04(12)	2112.0(5)	1529.2(6)
Z	4	4	2	4	4
ρ_{calc}, Mg/m^3	1.327	1.645	1.448	1.320	1.857
μ, mm^{-1}	1.349	1.541	1.404	1.193	1.700
F(000)	784	1688	404	880	848
cryst size, mm^3	0.50 × 0.30 × 0.15	0.50 × 0.50 × 0.20	0.50 × 0.20 × 0.20	1.10 × 0.60 × 0.10	0.30 × 0.20 × 0.10
θ range, °	2.58−26.80	1.96−26.50	2.65−28.45	1.52−28.29	2.10−28.38
hkl ranges	$-11 \le h \le 11$	$-19 \le h \le 19$	$-10 \le h \le 10$	$-17 \le h \le 17$	$-13 \le h \le 11$
	$-14 \le k \le 15$	$-17 \le k \le 17$	$-10 \le k \le 10$	$-15 \le k \le 15$	$-10 \le k \le 10$
	$-18 \le l \le 19$	$-21 \le l \le 21$	$-19 \le l \le 19$	$-17 \le l \le 17$	$-26 \le l \le 25$
reflns collected	6412	52 984	14 714	34 917	10 493
independent reflns	1790	6977	4169	9873	3503
R(int)	0.0326	0.0229	0.0176	0.0332	0.0327
completeness to φ	92.7%	100.0%	95.5%	96.8%	91.3%
max. and min. transmission	0.8233 and 0.5520	0.7481 and 0.5130	0.7666 and 0.5404	0.8900 and 0.3535	0.8484 and 0.6296
data/restraints/params	1790/0/134	6977/0/672	4169/2/297	9873/2/513	3503/0/286
GOF on F^2	1.000	1.048	1.033	1.028	1.022
final R indices [$I > 2\sigma(I)$]	R1 = 0.0382, wR2 = 0.0925	R1 = 0.0297, wR2 = 0.0774	R1 = 0.0274, wR2 = 0.0689	R1 = 0.0453, wR2 = 0.1184	R1 = 0.0458, wR2 = 0.1117
R indices (all data)	R1 = 0.0444, wR2 = 0.0962	R1 = 0.0367, wR2 = 0.0809	R1 = 0.0277, wR2 = 0.0691	R1 = 0.0505, wR2 = 0.1222	R1 = 0.0712, wR2 = 0.1236
absolute structure param	0.03(3)		0.004(7)	−0.005(12)	
largest diff. peak and hole, e Å^{-3}	0.490, −0.248	0.397, −0.169	0.569, −0.221	0.789, −0.465	0.980, −0.516

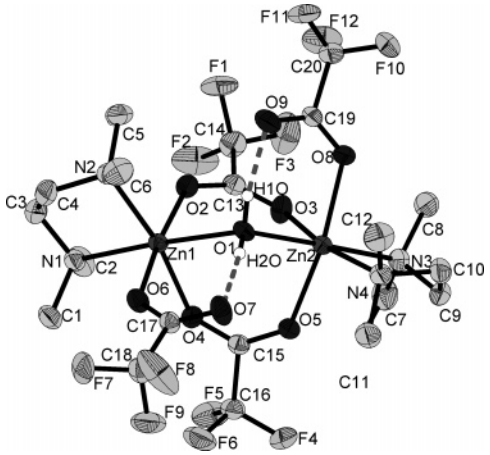

Figure 6. X-ray crystal structure of **4**.

is distorted tetrahedral[25] and in contrast to **1**, where the acetates are bidentate chelating, in **5** they are clearly monodentate. Like **5**, complex **6** is distorted tetrahedral with slight distortion of the metal−ligand angles from 109°. Both crotonates are clearly monodentate with bond lengths of Zn1−O1 = 1.988(14) Å, Zn1−O2 = 2.645(2) Å, Zn1−O3 = 1.973(15) Å, Zn1−O4 = 2.921(2) Å. The bonded Zn−O distances are only slightly different from those in **5**, which are 1.964 and 1.990 Å. The structure of **6** also contains a water molecule and extensive hydrogen bonding. Complexes **7** and **8** are also distorted tetrahedral with monodentate carboxylates. Tables of bond lengths and angles are available in the Supporting Information.

2. Structural Models for Hydroxamate Inhibition of Zinc Hydrolases. The dinuclear hydrolase structural models $[M_2(\mu\text{-}O_2CR)_2(O_2CR)_2(\mu\text{-}H_2O)(tmen)_2]$ (M = Ni, Co, Mn; R = CH_3, $C(CH_3)_3$), react with hydroxamic acids to give the hydroxamate bridged complexes $[M_2(\mu\text{-}O_2CR)(R'A)_2(tmen)_2][O_2CR]$, which closely model the inhibited hydrolases, e.g., urease. In view of this, the reactions of the aforementioned zinc complexes with hydroxamic acids were studied and the resulting complexes compared to hydroxamate inhibited zinc hydrolases, such as those involved in cancer progression and antibiotic resistance.

2.1. Reactions of the Mononuclear Complexes 1 and 2 with Acetohydroxamic Acid (AHA) and BHA. The reactions of the mononuclear zinc complexes **1** and **2** with AHA and BHA did not produce hydroxamate dibridged complexes analogous to $[M_2(\mu\text{-}O_2CR)_2(O_2CR)_2(\mu\text{-}H_2O)(tmen)_2]$ (M = Ni, Co, Mn; R = CH_3, $C(CH_3)_3$). Instead, neutral dinuclear complexes of general formula $[Zn_2(O_2CR)_3(tmen)(R'A)]$ were formed, i.e., **9**, **10**, **13**,[24] and **14** (Figure 7), in which the two zinc ions are bridged by a single hydroxamate and by two bridging bidentate carboxylates. The first zinc ion has a coordination number of six, with a capping tmen ligand, and the second zinc ion has a coordination number of four, and instead of a tmen ligand, there is a monodentate carboxylate bound. Hence, the introduction of a hydroxamic acid has induced dinuclearity in the complex. The 'dangling' oxygen

(25) (a) Chen, X.-M.; Xu, Z.-T.; Huang, X.-C. *J. Chem. Soc., Dalton Trans.* **1994**, 2331−2332. (b) Chen, X.-M.; Ye, B.-H.; Huang, X.-C.; Xu, Z.-T. *J. Chem. Soc., Dalton Trans.* **1996**, 3465−3468.

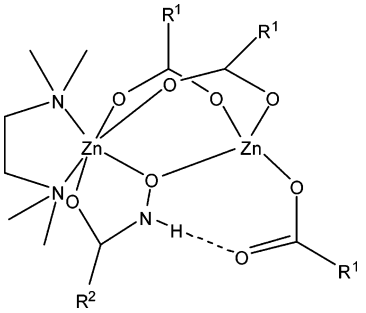

Figure 7. General structures of complexes **9**−**11** and **13**−**15**. Key: **9** (R^1 = CH_3, R^2 = CH_3), **10** (R^1 = $(CH)_2CH_3$, R^2 = CH_3), **11** (R^1 = $C(CH_3)_3$, R^2 = CH_3), **13** (R^1 = CH_3, R^2 = C_6H_5), **14** (R^1 = $(CH)_2CH_3$, R^2 = C_6H_5), **15** (R^1 = $C(CH_3)_3$, R^2 = C_6H_5).

of the monodentate carboxylate is hydrogen-bonded to the NH group of the acetohydroxamate. This zinc hydroxamate model complex, $[Zn_2(O_2CR)_3(tmen)(R'A)]$, shares many important structural features with *p*-iodo-D-phenylalanine hydroxamic acid inhibited *Aeromonas proteolytica* aminopeptidase.[18] Both are dinuclear, with a bidentate bridging carboxylate (aspartate in the enzyme) and a bridging hydroxamate. Significantly, they both share a similarity between the hydrogen bonding from the monodentate acetate to the NH of the hydroxamate in the model complex and the hydrogen bonding from the monodentate Glu151 in the enzyme. In all reactions with BHA, the side product $[Zn(BA)_2]\cdot H_2O$ (BA = benzohydroxamate) is produced, which is amorphous, highly insoluble, and probably polymeric.

2.2. Reactions of the Dinuclear Complexes 3 and 4 with AHA and BHA. Given that **3** and **4** have structures analogous to the Ni, Co, and Mn model dinuclear complexes, it was expected that, on reaction with AHA and BHA, the bis-hydroxamate-bridged dinuclear complex $[Zn_2(piv)(tmen)_2(R'A)_2][piv]$ (piv = $(CH_3)_3CCO_2^-$)[22] and the trinuclear $[Zn_3(OAc_F)_4(tmen)_2(R'A)_2]$[23] would form, analogous to those formed with Ni, Co, and Mn. However, the reactions of **3** with both AHA and BHA gave a product of general formula $[Zn_2(O_2CR)_3(tmen)(R'A)]$, i.e., **11** and **15** (Figure 7), both of which are analogous in structure to complexes **9**, **10**, **13**, and **14**. When **4** was reacted with AHA, instead of producing the expected $[Zn_3(OAc_F)_4(tmen)_2(AA)_2]$ (AA = acetohydroxamate), the dinuclear complex **12** (Figure 8) was formed. This complex is analogous in structure to complexes **9**−**11** and **13**−**15** except that in this case there are two tmen ligands. Consequently, both of the zinc atoms are six-coordinate.

The reaction of **4** with BHA produced the trinuclear complex **16** (Figure 8) as expected, with proton transfer to the nitrogen atoms of excess tmen and formation of the doubly protonated salt, $[tmenH_2][OAc_F]_2$.[23] This is the *only* reaction of the zinc model complexes with hydroxamic acids, which produces exactly the same result as the analogous Ni and Co reactions. The proposed mechanism for the formation of the trinuclear complex **16** is as follows. The dinuclear complex **4** reacts with 2 equiv of BHA to form the bis-benzohydroxamate chelate $[Zn(BA)_2]\cdot H_2O$, with the transfer of the hydroxamic protons to tmen to form $[tmenH_2][OAc_F]_2$ (Step A). One equivalent of $[Zn(BA)_2]\cdot H_2O$ then

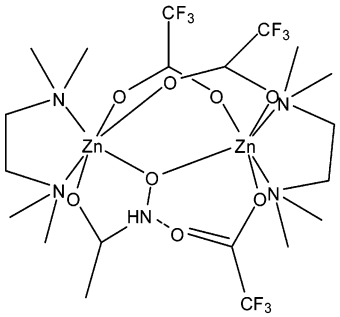

12

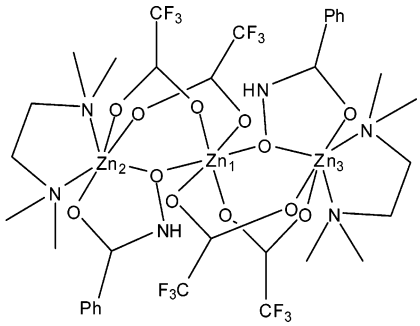

16

Figure 8. General structure of complexes **12** and **16**.

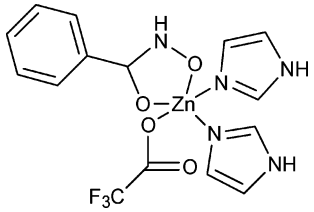

Figure 9. Structure of the mononuclear complex **17**.

reacts with the remaining **4** to form the trinuclear complex **16**.

Step A: 2 equiv **4** + 4BHA →
$2[Zn(BA)_2]\cdot H_2O + 2[tmenH_2][OAc_F]_2 + \mathbf{4}$

Step B: $\mathbf{4} + [Zn(BA)_2]\cdot H_2O \rightarrow \mathbf{16}$

Overall Reaction: 2 equiv **4** + 4BHA →
$2[Zn(BA)_2]\cdot H_2O + 2[tmenH_2][OAc_F]_2 + \mathbf{16}$

2.3. Reaction of Imidazole Complex 8 with BHA. In contrast to the reaction of $[M_2(\mu\text{-}O_2CR)_2(O_2CR)_2(\mu\text{-}H_2O)(Im)_4]$ with hydroxamic acid to give the hydroxamate complex $[M_2(O_2CR)(R'A)_2(Im)_4][O_2CR]$ (M = Ni, Co, Mn),[22] the reaction of the mononuclear imidazole complex **8** with BHA gave the mononuclear complex **17** (Figure 9). The complex is five-coordinate with distorted trigonal bipyramidal geometry around zinc. The benzohydroxamate is bidentate chelating in the 'O,O' mode, i.e., through the carbonyl oxygen and through the deprotonated hydroxamate OH. The mononuclear complex **17** is stoichiometrically half of the expected dinuclear complex $[Zn_2(OAc_F)(BA)_2(Im)_4][OAc_F]$. It is possible that the dinuclear complex formed first but then partially dissociated to the more stable neutral mononuclear complex **17**. The model complex bears a close similarity to the structure of thermolysin inhibited by L-Leu-NHOH hydroxamic acid.[11]

2.4. Reactions with $GluH_2A_2$. When $[M_2(\mu\text{-}O_2CR)_2(O_2CR)_2(\mu\text{-}H_2O)(tmen)_2]$ (M = Ni, Co and R = CH_3, $C(CH_3)_3$) is reacted with 1 equiv of $GluH_2A_2$, in the presence of a counterion, the ion $[M_2(O_2CR)\{\mu\text{-}O(N)(OC)_2(CH_2)_3\}(tmen)_2]^+$ is formed, with elimination of hydroxylamine.[20] However, there is no reaction between either **1** or **2** with $GluH_2A_2$, and the reactions of **3** and **4** with $GluH_2A_2$ produce a tetranuclear complex of general formula $[Zn_4(O_2CR)_6(tmen)_4(GluA_2)]$, i.e., **18** and **19** (Figure 10). These complexes have a different structure to the tetranuclear ion $[M_4(O_2CR)_2(GluA_2)_2(tmen)_4]^{2+}$, which was formed from the reaction of the urea complex $[M_2(O_2CR)_3(urea)(tmen)_2]$ with $GluH_2A_2$ (M = Ni, Co).[20]

2.5. Reactions with *N*-Methylbenzohydroxamic Acid (NMeBHA) and *N*-Phenylbenzohydroxamic Acid (NPhBHA). The hydrogen bonding between the NH of the hydroxamate ligand and the dangling oxygen of the monodentate carboxylate in the complexes **9**−**15**, **18**, and **19** has not been observed previously in the analogous Ni, Co, Mn complexes. To test the importance of this hydrogen bond in the formation of dinuclear zinc hydroxamate complexes, the model hydrolases **1**−**4** were reacted with the N-substituted hydroxamic acids, NMeBHA and NPhBHA, thus eliminating the availability of the NH proton. If dinuclear complexes were produced, then it may be concluded that the H-bonding between the hydroxamate NH and monodentate carboxylate is not a factor in dinuclear complex formation. However, when **1**−**4** were reacted with the N-substituted hydroxamic acids, all of the hydroxamic acid was converted into $[Zn(R'A)_2]$ and the remaining unreacted model hydrolase was recovered. Both $[Zn(NMeBA)_2]$ (NMeBA = *N*-methylbenzohydroxamate) and $[Zn(NPhBA)_2]$ (NPhBA = *N*-phenylbenzohydroxamate) are highly insoluble, amorphous, and most likely polymeric, similar to $[Zn(BA)_2]\cdot H_2O$. It is important to note that the reaction of $[M_2(\mu\text{-}O_2CR)_2(O_2CR)_2(\mu\text{-}H_2O)(tmen)_2]$ (M = Ni, Co; R = CH_3, $C(CH_3)_3$) with *N*-phenylacetohydroxamic acid does produce the dinuclear complex $[M_2(O_2CR)(NPhAA)_2(tmen)_2]^+$ (NPhAA = *N*-phenylacetohydroxamate),[22] thus suggesting that the presence of the NH proton and the hydrogen bond is only important when M = Zn.

2.6. Dinuclear Complexes 9−**11.** Crystallographic data for complexes **9**−**11** are shown in Table 2. Selected bond

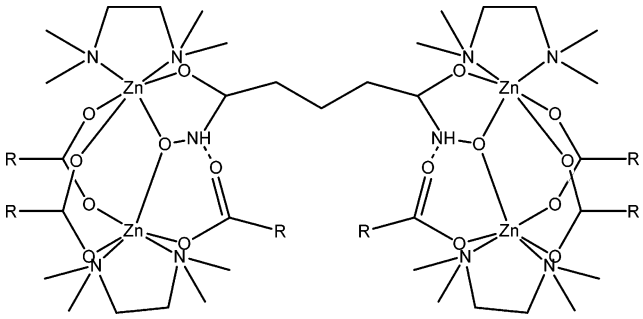

Figure 10. General structure of **18** (R = $C(CH_3)_3$) and **19** (R = CF_3).

Table 2. Crystal Data and Structure Refinement for Compounds **9**−**12**, **16**, **17**, and **19**

	9	**10**	**11**	**12**
empirical formula	$C_{28}H_{60}N_6O_{17}Zn_4$	$C_{20}H_{35}N_3O_8Zn_2$	$C_{23}H_{47}N_3O_8Zn_2$	$C_{20}H_{36}N_5O_8F_9Zn_2$
molecular formula	$C_{14}H_{29}N_3O_8Zn_4{\cdot}xH_2O$			
fw	1014.30	576.25	624.38	776.28
T, K	293(2)	100(2)	100(2)	293(2)
λ	0.71073	0.71073	0.71073	0.71073
cryst syst	monoclinic	triclinic	monoclinic	monoclinic
space group	*C*2/*c* (no. 15)	$P\bar{1}$ (no. 2)	$P2_1/n$ (no. 14)	$P2_1/c$ (no. 14)
a, Å	27.093(4)	11.3637(8)	9.0134(6)	12.9946(9)
b, Å	9.8118(16)	16.1153(11)	15.8999(11)	16.0297(12)
c, Å	16.806(3)	16.2312(11)	21.8147(15)	15.7070(11)
α, °	90	108.9900(10)	90	90
β, °	91.261(3)	104.8370(10)	100.240(1)	98.6990(10)
γ, °	90	99.1990(10)	90	90
V, Å^3	4466.3(13)	2619.0(3)	3076.5(4)	3234.1(4)
Z	4	4	4	4
ρ_{calc}, Mg/m^3	1.508	1.461	1.348	1.594
μ, mm^{-1}	2.191	1.877	1.603	1.582
F(000)	2104	1200	1320	1584
cryst size, mm^3	2.00 × 1.00 × 0.50	0.70 × 0.50 × 0.40	0.80 × 0.60 × 0.05	0.40 × 0.30 × 0.30
θ range, °	1.50−28.31	1.92−28.51	1.90−28.51	1.83−25.00
hkl ranges	$-35 \le h \le 35$	$-14 \le h \le 15$	$-12 \le h \le 12$	$-15 \le h \le 15$
	$-12 \le k \le 12$	$-21 \le k \le 21$	$-21 \le k \le 21$	$-19 \le k \le 19$
	$-22 \le l \le 22$	$-21 \le l \le 21$	$-28 \le l \le 29$	$-18 \le l \le 18$
reflns collected	36 569	22 466	51 471	22 803
independent reflns	5336	11 758	7412	5702
R(int)	0.0319	0.0152	0.0315	0.0263
completeness to φ max	96.0%	88.3%	94.8%	99.9%
max. and min. transmission	0.4071 and 0.0968	0.5206 and 0.3533	0.9241 and 0.3603	0.6482 and 0.5702
data/restraints/params	5336/0/366	11 758/0/619	7412/0/513	5702/0/494
GOF on F^2	1.042	1.045	1.055	1.032
final *R* indices [$I > 2\sigma(I)$]	R1 = 0.0277, wR2 = 0.0702	R1 = 0.0406, wR2 = 0.1050	R1 = 0.0254, wR2 = 0.0640	R1 = 0.0343, wR2 = 0.0870
R indices (all data)	R1 = 0.0357, wR2 = 0.0732	R1 = 0.0451, wR2 = 0.1079	R1 = 0.0288, wR2 = 0.0659	R1 = 0.0434, wR2 = 0.0930
largest diff. peak and hole, e Å^{-3}	0.477, −0.297	2.426, −1.231	0.547, −0.323	0.521, −0.281

	16	**17**	**19**
empirical formula	$C_{38}H_{54}N_6O_{13}F_{12}Zn_3$	$C_{15}H_{14}N_5O_4F_3Zn$	$C_{41}H_{72}N_{10}O_{16}F_{18}Zn_4$
molecular formula			
fw	1226.98	450.68	1564.57
T, K	100(2)	100(2)	100(2)
λ	0.71073	0.71073	0.71073
cryst syst	monoclinic	monoclinic	triclinic
space group	$P2_1/n$ (no. 14)	$P2_1$ (no. 4)	$P\bar{1}$ (no. 2)
a, Å	12.214(3)	10.2243(6)	10.6896(14)
b, Å	32.725(7)	7.9968(5)	17.774(2)
c, Å	12.878(3)	11.1919(7)	18.031(2)
α, °	90	90	65.562(2)
β, °	92.736(3)	97.290(1)	83.930(2)
γ, °	90	90	88.327(2)
V, Å^3	5141.5(19)	907.67(10)	3101.1(7)
Z	4	2	2
ρ_{calc}, Mg/m^3	1.585	1.649	1.676
μ, mm^{-1}	1.494	1.415	1.651
F(000)	2504	456	1596
cryst size, mm^3	1.00 × 0.90 × 0.60	0.40 × 0.40 × 0.10	0.20 × 0.20 × 0.05
θ range, °	2.33−27.00	1.83−28.53	1.26−23.00
hkl ranges	$-15 \le h \le 15$	$-13 \le h \le 13$	$-11 \le h \le 11$
	$-41 \le k \le 41$	$-10 \le k \le 10$	$-19 \le k \le 19$
	$-16 \le l \le 16$	$-14 \le l \le 14$	$-19 \le l \le 19$
reflns collected	39 493	15 513	18 516
independent reflns	11 164	4231	8551
R(int)	0.0449	0.0239	0.0356
completeness to φ max	99.5%	94.3%	99.1%
max. and min. transmission	0.4675 and 0.3165	0.8714 and 0.7407	0.9220 and 0.7181
data/restraints/params	11 164/0/740	4231/1/257	8551/0/826
GOF on F^2	1.166	1.046	1.089
final *R* indices [$I > 2\sigma(I)$]	R1 = 0.0639, wR2 = 0.1366	R1 = 0.0319, wR2 = 0.0808	R1 = 0.0448, wR2 = 0.1150
R indices (all data)	R1 = 0.0744, wR2 = 0.1408	R1 = 0.0326, wR2 = 0.0813	R1 = 0.0634, wR2 = 0.1245
largest diff. peak and hole, e Å^{-3}	1.070, −1.059	1.441, −0.255	1.011, −0.653

lengths and angles and figures are contained in the Supporting Information. The crystal structure of **13** has been previously reported,[24] and crystals of **14** and **15** were not suitable for X-ray crystallographic analysis. The X-ray crystal

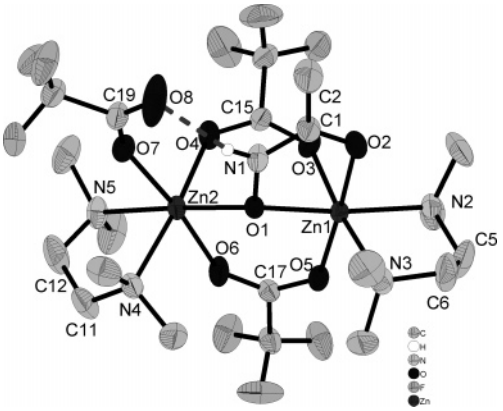

Figure 11. X-ray crystal structure of **12**. Hydrogens are omitted for clarity.

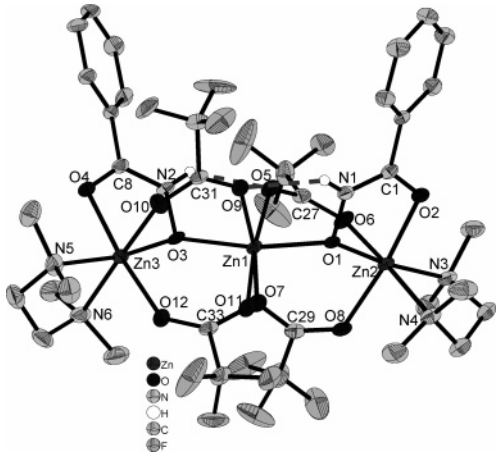

Figure 12. X-ray crystal structure of **16**.

structures of **9**−**11** reveal dinuclear complexes where Zn1 is four-coordinate and Zn2 is six-coordinate and thus analogous in structure to the previously reported **13**,[24] except that in these cases, acetohydroxamate is in place of benzohydroxamate.

2.7. X-ray Crystal Structure of 12. The X-ray crystal structure of **12** (Figure 11) reveals that it is similar to the structures of the previously described complexes **9**−**11** and **13**−**15**, i.e., it is dinuclear, with two bidentate bridging trifluoroacetates and one bridging hydroxamate, the NH of which is hydrogen bonded to a monodentate trifluoroacetate on Zn2. However, in this case, there are *two* tmen ligands, one on each zinc atom. Therefore, the coordination environment of both zinc atoms is distorted octahedral, with angles ∠O2−Zn1−N3 = 91.71(11)°, ∠O3−Zn1−O5 = 89.61(10)°, ∠N2−Zn1−O3 = 89.69(9)°, ∠O4−Zn2−O6 = 91.80(10)°, ∠O1−Zn2−O4 = 90.62(8)°, and ∠N4−Zn2−O7 = 90.16(9)°. The hydroxamate is coordinated in the bridging mode. The carbonyl oxygen, O2, coordinates to Zn1 (O2−Zn1 = 2.050(2) Å) and the hydroxamate oxygen, O1, bridges the two zinc atoms (O1−Zn1 = 2.106(18), O1−Zn2 = 2.075(17) Å). This is an asymmetric bridge, across a Zn−Zn separation of 3.609(1) Å. The bridging angle ∠Zn1−O1−Zn2 is 119.33(8)°. The two metal centers are also bridged by two bidentate bridging trifluoroacetates, with bond lengths Zn1−O3 = 2.175(2) Å, Zn1−O5 = 2.056(2) Å, Zn2−O4 = 2.094(2) Å, and Zn2−O6 = 2.149(2) Å and angles ∠O3−C15−O4 = 131.4(3)° and ∠O5−C17−O6 = 130.20(3)°. A third trifluoroacetate is coordinated monodentate to Zn2 (Zn2−O7 = 2.127(2) Å, Zn2−O8 = 3.832(5) Å). The noncoordinated or 'dangling' oxygen, O8, is hydrogen bonded to the NH of the hydroxamate (O8···H(N1) = 2.032(4) Å). Finally, there is a capping tmen on Zn1 (Zn1−N2 = 2.195(2) Å, Zn1−N3 = 2.232(3) Å) and on Zn2 (Zn2−N4 = 2.211(3) Å, Zn2−N5 = 2.241(2) Å). Selected bond lengths and angles can be found in the Supporting Information.

2.8. X-ray Crystal Structure of the Trinuclear Complex 16. The X-ray crystal structure of **16** (Figure 12) reveals that the complex is trinuclear and approximately linear (∠Zn2−Zn1−Zn3 = 169.31(2)°), where Zn1 is the central metal atom. The Zn−Zn separations are as follows. Zn1−Zn2 = 3.505(2) Å, Zn1−Zn3 = 3.524(2) Å, and Zn2−Zn3 = 6.999 Å. There are two capping tmen ligands, one each on Zn2 (Zn2−N3 = Zn2−N4 = 2.168(3) Å) and Zn3 (Zn3−N5 = 2.164(4) Å, Zn3−N6 = 2.162(4) Å). Bridging Zn1 and Zn2 are two bidentate bridging trifluoroacetates (Zn1−O5 = 2.167(3) Å, Zn1−O7 = 2.079(3) Å, Zn2−O6 = 2.180(3) Å, Zn2−O8 = 2.113(3) Å, ∠O5−C27−O6 = 131.3(4)°, ∠O7−C29−O8 = 130.9(4)°). A second pair of bidentate bridging trifluoroacetates bridge Zn1 and Zn3 (Zn1−O9 = 2.147(3) Å, Zn1−O11 = 2.062(3) Å, Zn3−O10 = 2.166(3) Å, Zn3−O12 = 2.094(3) Å, ∠O9−C31−O10 = 130.9(4)°, ∠O11−C33−O12 = 131.2(4)°). Also bridging Zn1 and Zn2 is a benzohydroxamate, coordinated in the bridging mode as previously observed. The carbonyl oxygen, O2, coordinates to Zn2 (O2−Zn2 = 2.083(3) Å) and the hydroxamate oxygen, O1, bridges the two zinc atoms (O1−Zn2 = 2.081(3) Å, O1−Zn1 = 2.057(3) Å). The bridging angle ∠Zn1−O1−Zn2 is 115.78(14)°. A second benzohydroxamate bridges Zn1 and Zn3. The carbonyl oxygen, O4, coordinates to Zn3 (O4−Zn3 = 2.120(3) Å), and the hydroxamate oxygen, O3, bridges the two zinc atoms (O3−Zn3 = 2.068(3) Å, O3−Zn1 = 2.074(3) Å). The bridging angle ∠Zn1−O3−Zn3 is 116.58(13)°. The complex is clearly unsymmetrical. There are no monodentate trifluoroacetates as observed in previous complexes. The distances O5···H(N2) = 2.098(5) Å and O9···H(N1) = 2.195(5) Å indicate that some interaction may exist between the NH of the hydroxamates and the bridging bidentate trifluoroacetates.

2.9. X-ray Crystal Structure of the Mononuclear Complex 17. The X-ray crystal structure of **17** (Figure 13) reveals that the complex is mononuclear with distorted trigonal bipyramidal geometry around the zinc. The zinc-bonded oxygen of the monodentate trifluoroacetate, O3, and the carbonyl oxygen of the hydroxamate, O2, are the axial atoms with an angle ∠O2−Zn1−O3 = 163.33(7)°. The two zinc-bound nitrogens of the imidazoles, N2 and N4, and the hydroxamate oxygen, O1, are equatorial with angles ∠N2−Zn1−N4 = 104.92(8)°, ∠O1−Zn1−N2 = 113.17(8)°, and ∠O2−Zn1−N4 = 93.20(8)°. The trifluoroacetate is bound to zinc in a monodentate fashion with Zn−O distances of Zn1−O3 = 2.108(17) Å and Zn1−O4 = 3.103(2) Å. The hydroxamate is in bidentate chelating 'O,O' mode with Zn−O distances of Zn1−O1 = 1.988(17) Å and Zn1−O2

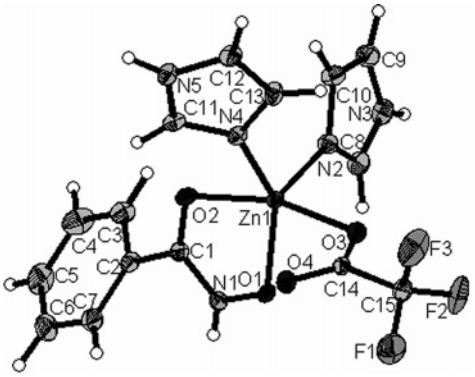

Figure 13. X-ray crystal structure of **17**.

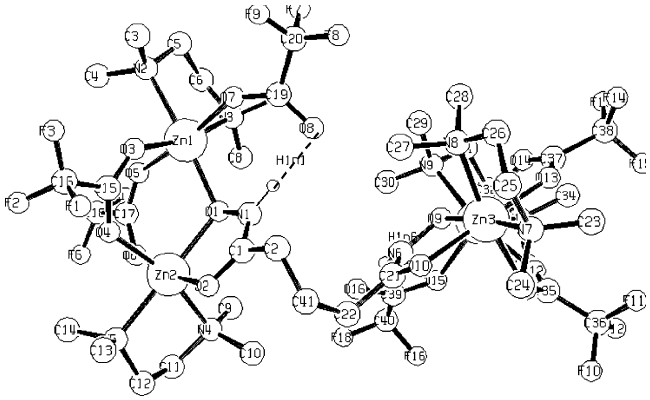

Figure 14. X-ray crystal structure of **19**.

= 2.189(17) Å. The Zn−N distances to the imidazoles are Zn1−N2 = 2.021(2) Å and Zn1−N4 = 2.002(2) Å. Individual units of **17** are linked to one another by three hydrogen bonds, O1···H(N5) = 1.852 Å, O2···H(N3) = 1.887 Å, and O4···H(N1) = 2.086(4) Å.

2.10. X-ray Crystal Structure of the Tetranuclear Complex 19. The X-ray crystal structure of **19** (Figure 14) reveals that the complex is tetranuclear and is composed of two dinuclear $[Zn_2(OAc_F)_3(tmen)_2(GluA_2)_{0.5}]$ units linked by the aliphatic chain of the $GluA_2$. $GluH_2A_2$ is a dihydroxamic acid with two hydroxamate functionalities linked by a $-(CH_2)_3-$ chain. The Zn−Zn separations in **19** are Zn1−Zn2 = 3.609(4) Å and Zn3−Zn4 = 3.600(3) Å. There is a separation of 8.741(3) Å between Zn1 and Zn3 and of 8.39(1) Å between Zn2 and Zn4. Selected dihedral angles are ∠Zn1−Zn2−Zn4−Zn3 = 93.13(2)° and ∠Zn2−Zn1−Zn3−Zn4 = 91.66(2)°. The general structure of each of the dinuclear units is similar to that of **12**, with the two zinc atoms bridged by two bidentate bridging trifluoroacetates and one hydroxamate, two capping tmen ligands and a monodentate trifluoroacetate with hydrogen bonding to the NH of the hydroxamate. All four zinc atoms are in a distorted octahedral environment with selected angles as follows. ∠O3−Zn1−O5 = 95.03(15)°, ∠O1−Zn2−O4 = 92.66(14)°, ∠N7−Zn3−O10 = 93.94(16)°, and ∠O12−Zn4−O15 = 92.53(14)°. Bridging Zn1 and Zn2 are two bidentate bridging trifluoroacetates (Zn1−O3 = 2.084(4) Å, Zn1−O5 = 2.127(4) Å, Zn2−O4 = 2.131(4) Å, Zn2−O6 = 2.078(4) Å, ∠O3−C15−O4 = 131.6(5)°, ∠O5−C17−O6 = 131.0(5)°). A second pair of bidentate bridging trifluoroacetates bridge Zn3 and Zn4 (Zn3−O11 = 2.164(4) Å, Zn3−O13 = 2.082(4) Å, Zn4−O12 = 2.096(4) Å, Zn4−O14 = 2.153(4) Å, ∠O11−C35−O12 = 130.9(5)°, ∠O13−C37−O14 = 129.4(5)°). One hydroxamate end of the $GluA_2$ bridges Zn1 and Zn2, and the other bridges Zn3 and Zn4, both coordinated in the bridging mode as previously observed. The carbonyl oxygen of the first end of the hydroxamate, O2, coordinates to Zn2 (O2−Zn2 = 2.073(4) Å) and the hydroxamate oxygen, O1, bridges the two zinc atoms (O1−Zn1 = 2.097(4) Å, O1−Zn2 = 2.131(4) Å). The bridging angle ∠Zn1−O1−Zn2 is 117.23(17)°. The carbonyl oxygen of the second end of the hydroxamate, O10, coordinates to Zn3 (O10−Zn3 = 2.083(4) Å) and the hydroxamate oxygen, O9, bridges the two zinc atoms (O9−Zn3 = 2.111(3) Å, O9−Zn4 = 2.069(4) Å). The bridging angle ∠Zn3−O9−Zn4 is 118.93(17)°. The complex is clearly unsymmetrical. There is one trifluoroacetate coordinated in a monodentate fashion on each of Zn1 (Zn1−O7 = 2.143(4) Å, Zn1−O8 = 3.798(6) Å) and Zn4 (Zn4−O15 = 2.130(4) Å, Zn4−O16 = 3.741(5) Å). Once again, the 'dangling' oxygens form a hydrogen bond to the NH of the hydroxamate (O8···H(N1) = 1.827(6) Å and O16···H(N6) = 2.023(6) Å). Finally, there are four capping tmen ligands, one on each on Zn1 (Zn1−N2 = 2.238(5) Å, Zn1−N3 = 2.240(5) Å), Zn2 (Zn2−N4 = 2.217(5) Å, Zn2−N5 = 2.197(5) Å), Zn3 (Zn3−N7 = 2.179(4) Å, Zn3−N8 = 2.241(5) Å), and Zn4 (Zn4−N9 = 2.231(4) Å, Zn4−N10 = 2.236(4) Å).

2.11. IR Spectroscopic Studies. A full list of IR peaks and assignments for all compounds studied is contained in the Supporting Information. The assignments for the bands observed in the IR spectra are based on both reported values for the zinc carboxylates[26−32] and our previous work.[19−24]

Experimental Section

Reagents and solvents were used as obtained from Sigma-Aldrich, UK, without further purification unless otherwise stated. The microanalytical laboratory, Chemical Services Unit, University College Dublin, performed elemental analyses. Infrared spectra were recorded in the solid state using 1−2% KBr disks and solutions in a calcium fluoride cell, path length 0.1 mm, using a Perkin-Elmer FT-IR Paragon 1000 or a Perkin-Elmer Spectrum One FT-IR spectrometer.

Preparation of Zinc Pivalate, $Zn(piv)_2$ and Zinc Crotonate, $Zn(crot)_2 \cdot H_2O$. A solution of the relevant carboxylic acid (100 mmol) in methanol was added slowly dropwise to a stirred suspension of zinc carbonate, $2ZnCO_3 \cdot 3Zn(OH)_2$ (10 mmol) in very hot water, taking care to vent carbon dioxide. The reaction mixture was allowed to stir for 48 h, after which it was filtered and the

(26) Johnson, M. K.; Powell, D. B.; Cannon, R. D. *Spectrochim. Acta* **1981**, *37A*, 899−904.
(27) Ishioka, T.; Shibata, Y.; Takahashi, M.; Kanesaka, I.; Kitagawa, Y.; Nakamura, K. T. *Spectrochim. Acta, Part A* **1998**, *54*, 1827−1836.
(28) Clegg, W.; Little, I. R.; Straughan, B. P. *Acta Crystallogr.* **1986**, *C42*, 1701−1703.
(29) Ishioka, T.; Shibata, Y.; Takahashi, M.; Kanesaka, I. *Spectrochim. Acta, Part A* **1998**, *54*, 1811−1818.
(30) Clegg, W.; Little, I. R.; Straughan, B. P. *Acta Crystallogr.* **1986**, *C42*, 919−920.
(31) Clegg, W.; Harbron, D. R.; Homan, C. D.; Hunt, P. A.; Little, I. R.; Straughan, B. P. *Inorg. Chim. Acta* **1991**, *186*, 51−60.
(32) Mehrotra, R. C.; Bohra, R. *Metal Carboxylates*; Academic Press: London, 1983.

filtrate left to stand in air for ~1 week to afford white $Zn(piv)_2$ [Yield: 8.2 g (61%). Anal. Calcd for $C_{10}H_{18}O_4Zn$: C, 44.88; H, 6.78; Zn, 24.43. Found: C, 44.71; H, 6.72; Zn, 24.30] or $Zn(crot)_2 \cdot H_2O$ [Yield: 18.5 g (73%). Anal. Calcd for $C_{32}H_{42}O_{18}Zn_5$: C, 36.90; H, 4.06; Zn, 31.39. Found: C, 36.80; H, 3.95; Zn, 30.03].

Preparation of 1−4. A solution of tmen (10 mmol) in methanol was added slowly dropwise to a stirred solution of the appropriate zinc carboxylate (10 mmol) in methanol. The reaction mixture was stirred for 3 h, and the solvent evaporated by standing in air to afford colorless crystals of **1**, **2**, **3**, or **4**, which were recrystallized from diethyl ether. Yield of **1**: 2.7 g, (81%). Anal. Calcd for $C_{10}H_{22}N_2O_4Zn$ (**1**): C, 40.08; H, 7.40; N, 9.35; Zn, 21.82. Found: C, 40.08; H, 7.38; N, 9.33; Zn, 20.71. Yield of **2**: 1.5 g, (43%). Anal. Calcd for $C_{14}H_{28}N_2O_5Zn$ (**2**): C, 46.61; H, 7.54; N, 7.77; Zn, 18.12. Found: C, 46.83; H, 7.38; N, 7.79; Zn, 19.71. Yield of (**3**): 2.8 g (35%). Anal. Calcd for $C_{32}H_{70}N_4O_9Zn_2$ (**3**): C, 48.92; H, 8.98; N, 7.13; Zn, 16.64. Found: C, 48.73; H, 8.93; N, 7.05; Zn, 16.25. Yield of **4**: 6.4 g (77%). Anal. Calcd for $C_{20}H_{34}N_4F_{12}O_9Zn_2$ (**4**): C, 28.83; H, 4.11; N, 6.72; F, 27.36; Zn, 15.69. Found: C, 28.80; H, 4.01; N, 6.60; F, 26.88; Zn, 15.14.

Preparation of 5−8. A solution of imidazole (20 mmol) in methanol was added slowly dropwise to a stirred solution of the appropriate zinc carboxylate (10 mmol) in methanol. The reaction mixture was stirred for 3 h, filtered, and the solvent evaporated by standing in air to afford colorless crystals of **5**, **6**, **7**, or **8**, which were recrystallized from diethyl ether. Yield of **5**: 2.1 g (66%). Anal. Calcd for $C_{10}H_{14}N_4O_4Zn$ (**5**): C, 37.58; H, 4.42; N, 17.53; Zn, 20.46. Found: C, 37.25; H, 4.29; N, 17.30; Zn, 20.29. Yield of **6**: 0.8 g (22%). Anal. Calcd for $C_{14}H_{20}N_4O_5Zn$ (**6**): C, 43.15; H, 5.17; N, 14.38; Zn, 16.78. Found: C, 42.92; H, 4.85; N, 14.20; Zn, 17.63. Yield of **7**: 2.3 g (58%). Anal. Calcd for $C_{16}H_{28}N_4O_5Zn$ (**7**): C, 46.56; H, 6.59; N, 13.57; Zn, 15.84. Found: C, 46.37; H, 6.45; N, 13.45; Zn, 14.21. Yield of **8**: 3.2 g (74%). Anal. Calcd for $C_{10}H_8N_4F_6O_4Zn$ (**8**): C, 28.09; H, 1.89; N, 13.10; F, 26.11; Zn, 14.98. Found: C, 28.70; H, 1.77; N, 14.45; F, 25.47; Zn, 15.35.

Preparation of the Hydroxamic Acids. Hydroxamic acids were prepared as described previously.[33,34]

Preparation of 9−12. A solution of AHA (10 mmol) in MeOH was added dropwise to a solution of **1**, **2**, **3**, or **4** (10 mmol) in MeOH and stirred for 1 h. The solution was concentrated under vacuum to produce an oil, which was stirred in ether, filtered, and the ether washings were left to stand in air to produce colorless crystals of **9**, **10**, **11**, and **12**, respectively. Yield of **9**: 1.1 g (22%). Anal. Calcd for $C_{14}H_{29}N_3O_8Zn_2$ (**9**): C, 33.76; H, 5.87; N, 8.44; Zn, 26.24. Found: C, 32.64; H, 5.87; N, 8.02; Zn, 26.72. Yield of **10**: 1.2 g (42%). Anal. Calcd for $C_{20}H_{35}N_3O_8Zn_2$ (**10**): C, 41.69; H, 6.12; N, 7.29; Zn, 22.69. Found: C, 41.66; H, 6.31; N, 7.29; Zn, 21.80. Yield of **11**: 1.6 g (51%). Anal. Calcd for $C_{23}H_{47}N_3O_8Zn_2$ (**11**): C, 44.24; H, 7.59; N, 6.73; Zn, 20.94. Found: C, 43.84; H, 7.45; N, 6.83; Zn, 19.84. Yield of **12**: 1.8 g (48%). Anal. Calcd for $C_{20}H_{26}N_5F_9O_6Zn_2$ (**12**): C, 30.95; H, 4.67; N, 9.02; F, 22.03; Zn, 16.84. Found: C, 30.10; H, 4.41; N, 8.54; F, 22.08; Zn, 16.27.

Preparation of 13−16. A solution of BHA (10 mmol) in MeOH was added dropwise to a solution of **1**, **2**, **3**, or **4** (10 mmol) in MeOH and stirred for 1 h. Almost immediately, $[Zn(BA)_2] \cdot H_2O$ formed as a white precipitate—an amorphous powder which is unsuitable for X-ray crystallographic analysis. The solution was filtered and the filtrate concentrated under vacuum to produce an oil, which was stirred in ether, filtered, and the ether washings left to stand in air to produce colorless crystals of **13**, **14**, **15**, and **16**, respectively. Yield of **13**: 0.8 g (14.3%). Anal. Calcd for $C_{19}H_{31}N_3O_8Zn_2$ (**13**): C, 40.73; H, 5.58; N, 7.50; Zn, 23.34. Found: C, 40.63; H, 5.57; N, 7.39; Zn, 22.94. Yield of **14**: 1.4 g (44%). Anal. Calcd for $C_{25}H_{37}N_3O_8Zn_2$ (**14**): C, 47.04; H, 5.84; N, 6.58; Zn, 20.48. Found: C, 47.01; H, 5.75; N, 6.54; Zn, 20.06. Yield of **15**: 0.9 g (26%). Anal. Calcd for $C_{28}H_{49}N_3O_8Zn_2$ (**15**): C, 48.99; H, 7.19; N, 6.12; Zn, 19.05. Found: C, 48.94; H, 7.24; N, 6.13; Zn, 20.04. Yield of **16**: 0.9 g (16%). Anal. Calcd for $C_{34}H_{44}N_6F_{12}O_{12}Zn_3$ (**16**): C, 35.42; H, 3.85; N, 7.29; F, 19.29; Zn, 17.01. Found: C, 35.23; H, 3.69; N, 6.99; F, 19.25; Zn, 17.43.

Preparation of 17. A solution of BHA (10 mmol) in MeOH was added dropwise to a solution of **8** (10 mmol) in MeOH and stirred for 1 h. The solution was filtered and the filtrate concentrated under vacuum to produce an oil, which was stirred in ether, filtered, and the *ether-insoluble* portion recrystallized from CH_2Cl_2 to produce colorless crystals of **17** suitable for X-ray crystallographic analysis. Yield: 2.7 g (60%). Anal. Calcd for $C_{15}H_{14}N_5F_3O_4Zn$: C, 39.96; H, 3.13; N, 15.54; F, 12.65; Zn, 14.51. Found: C, 39.56; H, 3.16; N, 15.02; F, 11.82; Zn, 13.90.

Preparation of 18 and 19. A solution of $GluH_2A_2$ (20 mmol) in MeOH was added dropwise to a solution of **3** or **4** (10 mmol) in MeOH and stirred for 1 h, filtered, and concentrated under vacuum. The resulting residue was stirred in ether, filtered, and the filtrate left to stand in air to produce colorless crystals of **18** or **19**, respectively. Yield of **18**: 2.1 g (28%). Anal. Calcd for $C_{59}H_{126}N_{10}O_{16}Zn_4$ (**18**): C, 47.46; H, 8.50; N, 9.38; Zn, 17.51. Found: C, 46.75; H, 8.06; N, 8.94; Zn, 16.82. Yield of **19**: 2.9 g (47%). Anal. Calcd for $C_{41}H_{72}N_{10}F_{18}O_{16}Zn_4$ (**19**): C, 31.48; H, 4.64; N, 8.95; F, 21.86; Zn, 16.72. Found: C, 30.40; H, 4.52; N, 8.35; F, 21.73; Zn, 15.79.

Crystal Structure Determinations. Crystallographic data for **2**, **4**, **6−12**, **16**, **17**, and **19** were collected using a Bruker D8 goniometer equipped with a Bruker SMART APEX CCD area detector and a Mo Kα X-ray tube. A full sphere of reciprocal space was scanned by $\varphi-\omega$ scans. Semiempirical absorption correction, based on redundant reflections, was performed by the program SADABS.[35] The structures were solved by direct methods using SHELXTL-PC[36] and refined by full matrix least-squares on F^2 for all data using SHELXL-97.[37] Anisotropic displacement parameters were refined for all non-hydrogen atoms.

The treatment of the hydrogen atoms varies from compound to compound, as crystal quality sometimes limited the options. Protons of water molecules of crystallization were either located in the difference Fourier map (**2**, **6**, **9**) or could not at all be detected (**7**). In **2**, the water proton (there is only one hydrogen site as the water molecule occupies a 2-fold axis) was refined riding on the oxygen atom, its isotropic displacement parameter fixed to 1.5 times the equivalent displacement parameter of the oxygen atom. In **6** and **9**, the water protons were refined freely including isotropic displacement parameters.

The following noncrystal-water hydrogen atoms were refined freely including isotropic displacement parameters: All of them in **4**, **6**, **8**, and **11**, the ordered ones in **2** and **9**, and those attached to nitrogen in **10**, **12**, **16**, **17**, and **19**. All remaining hydrogen atoms were added at calculated positions and refined using a riding model.

(33) Brown, D. A.; Roche, A. L. *Inorg. Chem.* **1983**, *22*, 2199.
(34) Brown, D. A.; Ní Choileáin, N.; Geraty, R. *Inorg. Chem.* **1986**, *25*, 3792.
(35) Sheldrick, G. M. *SADABS, Empirical Absorption Corrections Program*; University of Göttingen: Göttingen, Germany, 1996.
(36) *Siemens SHELXTL-PC Version 5.0, Reference Manual*; Siemens Industrial Automation, Inc., Analytical Instrumentation: Madison, WI, 1994.
(37) Sheldrick, G. M. *SHELXL97, Program for Crystal Structure Refinement*; University of Göttingen: Göttingen, Germany, 1997.

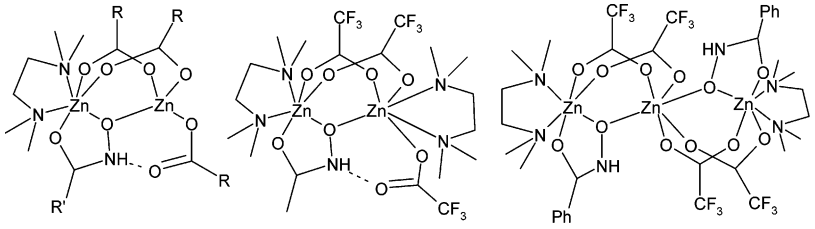

	Tmen	AHA	BHA	NMeBHA	NPhBHA	$GluH_2A_2$
OAc	Mononuclear complex	Dinuclear complex A	Dinuclear complex A	No rxn	No rxn	No rxn
Crot	Mononuclear complex	Dinuclear complex A	Dinuclear complex A	No rxn	No rxn	No rxn
Piv	Dinuclear complex	Dinuclear complex A	Dinuclear complex A	No rxn	No rxn	Tetranuclear complex
OAc_F	Dinuclear complex	Dinuclear complex B	Trinuclear complex	No rxn	No rxn	Tetranuclear complex

Figure 15. Summary of the reactions of the model complexes with hydroxamic acids.

Their isotropic displacement parameters were fixed to 1.2 times (1.5 times for methyl groups) the equivalent isotropic displacement parameters of the atom the H-atom is attached to.

Conclusions

We have shown that the bridging mode of coordinated hydroxamate as observed previously[15−24] is conserved in the multinuclear zinc−hydroxamate complexes described here. However, unlike the bis-hydroxamate bridged complexes $[M_2(\mu\text{-}O_2CR)(R'A)_2(tmen)_2][O_2CR]$ (M = Ni, Co, Mn; R = CH_3, $C(CH_3)_3$), the zinc−hydroxamate species contain only a single bridging hydroxamate. It is this singly bridging motif that is in fact observed in the X-ray crystal structures of hydrolases inhibited by hydroxamic acids.[16−18] The presence of hydrogen bonding between the dangling oxygen of the monodentate carboxylate and the NH of the hydroxamate in $[Zn_2(O_2CR)_3(tmen)(R'A)]$ may be important in the formation of the hydroxamate dinuclear complex, since the reactions of **1**, **2**, **3**, and **4** with the N-substituted hydroxamic acids failed to produce dinuclear hydroxamate complexes (Figure 15). The above H-bonding in $[Zn_2(O_2CR)_3(tmen)(R'A)]$ models closely that observed between the hydroxamate NH and the free oxygen of Glu151 in *Aeromonas proteolytica* aminopeptidase (Zn_2AAP) inhibited by *p*-iodo-D-phenylalanine hydroxamic acid.[18,24] $GluH_2A_2$ fails to react with the mononuclear **1** and **2**, but on reaction with the dinuclear **3** and **4**, the tetranuclear complexes **18** and **19** are formed (Figure 15), in contrast to the Ni and Co series where the reaction of $[M_2(O_2CR)_4(\mu\text{-}H_2O)(tmen)_2]$ (M = Ni, Co) with $GluH_2A_2$ gives the ion $[M_2(O_2CR)\{\mu\text{-}O(N)(OC)_2(CH_2)_3\}(tmen)_2]^+$, with elimination of hydroxylamine. It is probably the coordinative flexibility of the Zn^{2+} ion that allows the formation of the flexible neutral species $[Zn_4(O_2CR)_6(tmen)_4(GluA_2)]$ in preference to the highly strained cyclic ionic product $[M_2(O_2CR)\{\mu\text{-}O(N)(OC)_2(CH_2)_3\}(tmen)_2]^+$. While complexes **1**, **2**, and **3** all react in identical ways with AHA and BHA giving complexes of general formula $[Zn_2(O_2CR)_3(tmen)(R'A)]$, the reactions of **4** with AHA and BHA both produce different products. The reaction with AHA results in the formation of **15**, which is structurally very similar to the $[Zn_2(O_2CR)_3(tmen)(R'A)]$ complexes, with the exception of the second tmen ligand. The M−M separations for the complexes $[Zn_2(O_2CR)_3(tmen)(R'A)]$ (OAc, crot, piv) are all ∼3.2 Å, whereas the distance in the OAc_F complexes are all ∼3.6 Å.[23,24] This larger M−M separation in the trifluoroacetate complexes is caused by the larger size of the OAc_F ion. This, combined with the strongly electron withdrawing properties of the OAc_F ion, allows a second tmen ligand to coordinate to Zn2. In the BHA case, the added electron withdrawing power of the benzene ring on the hydroxamate allows two $[Zn_2(OAc_F)_3(tmen)(BA)]$ units to combine to form **16**, instead of simply adding a second tmen as in the case of **15**. Finally, care must be taken when using alternative metals to study the zinc enzymes, e.g., cobalt substitution.

Acknowledgment. We gratefully acknowledge support from the following bodies: EU COST D21 Project D21/0001/00; Centre for Synthesis and Chemical Biology, Conway Institute of Biomolecular and Biomedical Research, University College Dublin. We also thank Ms. Anne Connolly of the microanalytical laboratory, Chemical Services Unit, University College Dublin, who performed the elemental analyses.

Supporting Information Available: Tables of NMR and IR data for all complexes; CIF files for structures **2**, **4**, **6**, **7**, **8**, **9**, **10**, **11**, **12**, **16**, **17**, and **19**; and selected bond lengths and angles and ORTEP figures. This material is available free of charge via the Internet at http://pubs.acs.org.

IC050849M